Enhanced C−C Bond Formation of Heterodinuclear Methylplatinum−Molybdenum Complexes Having a Hemilabile Ligand with Dialkyl Acetylenedicarboxylate

Susumu Tsutsuminai, Nobuyuki Komine, Masafumi Hirano, and Sanshiro Komiya*

Department of Applied Chemistry, Faculty of Technology, Tokyo University of Agriculture and Technology, 2-24-16 Nakacho, Koganei, Tokyo 184-8588, Japan

Received September 9, 2003

Heterodinuclear methylplatinum−molybdenum complexes having a hemilabile P−L ligand, (P−L)MePt−MoCp(CO)$_3$ (P−L = $Ph_2PC_2H_4NEt_2$ (**1**), $Ph_2PC_2H_4CH{=}CH_2$ (**2**)), react with dialkyl acetylenedicarboxylate to afford the novel heterodinuclear complexes (P−L)MePt{μ-η^2:η^2-C(O)C$_2$(CO$_2$R)$_2$}MoCp(μ-CO)(CO) (P−L = $Ph_2PC_2H_4NEt_2$, R = Me (**5**); P−L = $Ph_2PC_2H_4CH{=}CH_2$, R = Me (**6**); P−L = $Ph_2PC_2H_4NEt_2$, R = Et (**7**)). An X-ray diffraction study of **5** has revealed that the complex has a unique structure containing a platinacyclobutenone framework, where the π-bond coordinates to the molybdenum. Heating of **5** at 50 °C for 2 days results in reductive elimination of methyl and alkenyl ligands followed by decarbonylation to form the new μ-alkenyl type complexes ($Ph_2PC_2H_4NEt_2$-κ^2N,P){μ-MeO$_2$C(Me)=CCO$_2$Me}Pt−MoCp(μ-CO)(CO) (**8**) and ($Ph_2PC_2H_4NEt_2$-κ^1P)(CO){μ-MeO$_2$C(Me)=CCO$_2$Me}Pt−MoCp(μ-CO)(CO) (**9**). Reactions of **5** with ^{t}BuNC or PMe_3 cause selective ligand displacement of the amino moiety in the P−N ligand to form ($Ph_2PC_2H_4NEt_2$-κ^1P)(L′)MePt{μ-η^2:η^2-C(O)C$_2$(CO$_2$Me)$_2$}MoCp(μ-CO)(CO) (L′ = ^{t}BuNC (**10**), PMe_3 (**11**)). On the other hand, nucleophiles such as H_2NBu, $HNEt_2$, pyrrolidine, and KOPh add to acyl carbon to give the trisubstituted μ-alkenyl type complexes ($Ph_2PC_2H_4NEt_2$-κ^2N,P)Me{μ-MeO$_2$C(R$_2$NCO)C=CCO$_2$Me}Pt−MoCp(μ-CO)(CO) (NR$_2$ = NHBu (**12**), NEt$_2$ (**13**), NC$_4$H$_8$ (**14**)) and K$^+$[($Ph_2PC_2H_4NEt_2$-κ^1P)Me{μ-MeO$_2$C(PhO$_2$C)C=CCO$_2$Me}Pt−MoCp(μ-CO)(CO)]$^-$ (**15**).

Introduction

Heterodinuclear complexes have attracted intrinsic interest due to their possible cooperative effect of two different metal centers in catalytic and stoichiometric chemical reactions.[1−3] Introduction of an unsymmetrical chelating ligand into such dinuclear complexes is expected to provide a highly selective reaction environment, because preferential partial dissociation of the chelating ligand gives a specific vacant coordination site on a metal center.[4] We recently reported the synthesis of hetrodinuclear organoplatinum complexes having a hemilabile P−N ligand (2-(diphenylphosphino)triethylamine), which show a facile and reversible Pt−N bond rupture causing high reactivity toward CO.[5] In the present study, we wish to report the synthesis of new heterodinuclear organoplatinum complexes with unsymmetrical P−olefin and P−S ligands and reactions of these heterodinuclear organoplatinum complexes with dimethyl acetylenedicarboxylate to give the novel μ-platinacyclobutenone complexes ($Ph_2PC_2H_4NEt_2$-κ^2N,P)MePt{μ-η^2:η^2-C(O)C$_2$(CO$_2$Me)$_2$}MoCp(μ-CO)(CO). Unique thermal transformation and nucleophilic reactions of these platinacyclobutenes to give heterodinuclear alkenylplatinum complexes are also described.

Results and Discussion

Synthesis of Heterodinuclear Methylplatinum−Molybdenum Complexes Having Unsymmetrical P−Olefin and P−S Ligands. We recently described

* To whom correspondence should be addressed. E-mail: komiya@cc.tuat.ac.jp.

(1) (a) Braunstein, P., Oro, L. A., Raithby, P. R., Eds. *Metal Clusters in Chemistry*; Wiley-VCH: Weinheim, Germany, 1999. (b) Adams, R. D., Cotton, F. A., Eds. *Catalysis by Di- and Polynuclear Metal Cluster Complexes*; Wiley-VCH: New York, 1998. (c) Chetcuti, M. J. In *Comprehensive Organometallic Chemistry II*; Adams, R. D., Ed.; Pergamon Press: Oxford, U.K., 1995; Vol. 10. (d) Shriver, D. F., Kaesz, H., Adams, R. D., Eds. *The Chemistry of Metal Cluster Complexes*; VCH: New York, 1990.

(2) (a) Braunstein, P.; Morise, X. *Organometallics* **1998**, *17*, 540. (b) Adams, R. D.; Barnard, T. S.; Wu, Z. Li. W.; Yamamoto, J. H. *J. Am. Chem. Soc.* **1994**, *116*, 9103. (c) Braunstein, P.; Knorr, M.; Stähreldt, J. *J. Chem. Soc., Chem. Commun.* **1994**, 1913.

(3) (a) Komiya, S.; Endo, I. *Chem. Lett.* **1988**, 1709. (b) Fukuoka, A.; Sadashima, T.; Endo, I.; Ohashi, N.; Kambara, Y.; Sugiura, T.; Komiya, S. *Organometallics* **1994**, *13*, 4033. (c) Fukuoka, A.; Sadashima, T.; Sugiura, T.; Wu, X.; Mizuho, Y.; Komiya, S. *J. Organomet. Chem.* **1994**, *473*, 139. (d) Fukuoka, A.; Sugiura, T.; Yasuda, T.; Taguchi, T.; Hirano, M.; Komiya, S. *Chem. Lett.* **1997**, 329. (e) Fukuoka, A.; Fukagawa, S.; Hirano, M.; Komiya, S. *Chem. Lett.* **1977**, 377. (f) Yasuda, T.; Fukuoka, A.; Hirano, M.; Komiya, S. *Chem. Lett.* **1998**, 29. (g) Komiya, S.; Muroi, S.; Furuya, M.; Hirano, M. *J. Am. Chem. Soc.* **2000**, *122*, 170. (h) Komine, N.; Hoh, H.; Hirano, M.; Komiya, S. *Organometallics* **2000**, *19*, 5251. (i) Fukuoka, A.; Fukagawa, S.; Hirano, M.; Koga, N.; Komiya, S. *Organometallics* **2001**, *20*, 2065.

(4) (a) Braunstein, P.; Naud, F. *Angew. Chem., Int. Ed.* **2001**, *40*, 680. (b) Anderson, G. K.; Lumetta, G. J. *Organometallics* **1985**, *4*, 1542. (c) Dekker, G. P. C. M.; Buijs, A.; Elsevier, C. J.; Vrieze, K.; Smeets, W. J. J.; Spek, A. L.; Wang, Y. F.; Stam, C. H. *Organometallics* **1992**, *11*, 1937. (d) Mauthner, K.; Slugovc, C.; Mereiter, K.; Schmid, R.; Kirchner, K. *Organometallics* **1997**, *16*, 1956. (e) Hayashi, T.; Kumada, M. *Acc. Chem. Res.* **1982**, *15*, 395. (f) Pfeiffer, J.; Kickelbick, G.; Schubert, U. *Organometallics* **2000**, *19*, 62. (g) Yoshida, H.; Shirakawa, E.; Kurahashi, T.; Nakao, Y.; Hiyama, T. *Organometallics* **2000**, *19*, 5671. (h) Müller, C.; Lachicotte, R. J.; Jones, W. D. *Organometallics* **2002**, *21*, 1975.

(5) Tsutsuminai, S.; Komine, N.; Hirano, M.; Komiya, S. *Organometallics* **2003**, *22*, 4238.

10.1021/om034162q CCC: $27.50
Publication on Web 12/06/2003

Scheme 1

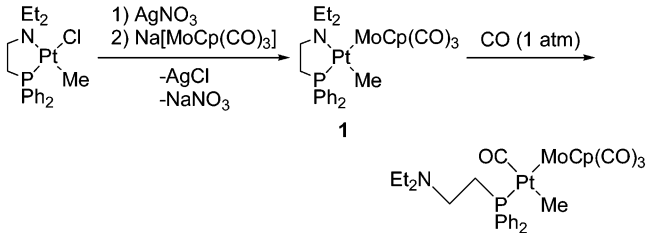

the synthesis of organoplatinum−molybdenum complexes having a P−N ligand, ($Ph_2PC_2H_4NEt_2$-κ^2N,P)MePt−$MoCp(CO)_3$ (**1**; Scheme 1), which showed dynamic behavior arising from facile reversible Pt−N bond rupture, and this hemilabile nature of the P−N ligand leads to high reactivity toward CO, causing facile ligand displacement of the N atom by CO to give ($Ph_2PC_2H_4NEt_2$-κ^1P)(CO)MePt−$MoCp(CO)_3$ with monodentate phosphorus coordination.[5]

In addition to the previously prepared complex **1**, novel platinum−molybdenum complexes having an unsymmetrical P−L bidentate ligand such as but-3-enyldiphenylphosphine[6] and 2-(diphenylphosphino)ethyl methyl sulfide[7] (P−L)MePt−$MoCp(CO)_3$ (P−L = $Ph_2PC_2H_4CH{=}CH_2$ (**2**), $Ph_2PC_2H_4SMe$ (**3**)) were newly prepared by the ligand exchange reaction of (cod)MePt−$MoCp(CO)_3$[3b] (eq 1) with $Ph_2PC_2H_4CH{=}CH_2$ as well as

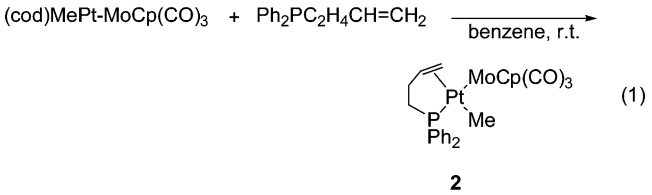

(1)

by metathetical reactions of $PtMe(NO_3)(Ph_2PC_2H_4SMe$-$\kappa^2P,S)$ with $Na[MoCp(CO)_3]$ (eq 2). They were characterized by NMR and IR spectroscopy and elemental analyses. The $^{31}P\{^1H\}$ NMR spectra of **2** and **3** show singlets at δ 42.0 and 57.4 with ^{195}Pt satellites having the large $^1J_{Pt-P}$ values 3584 and 3734 Hz, respectively, suggesting that the phosphorus atom of these ligands locates in a position trans to the $MoCp(CO)_3$ moiety similar to the previously prepared analogous complexes with the P−N ligand **1**. In the ^1H NMR spectra, the vinyl protons of the P−olefin ligand and the methyl protons of the P−S ligand are also observed with ^{195}Pt satellites. The data indicate that these ligands are coordinated to the Pt center in a bidentate fashion, but the ligand dissociation process is not fast enough to show dynamic behavior in NMR at ambient temperature.

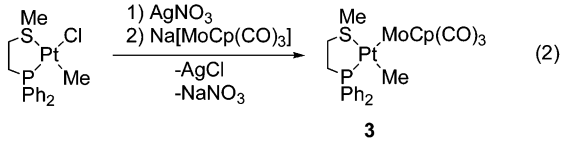

(2)

(6) (a) Hursthouse, M. B.; Malik, K. M. A. *Polyhedron* **1996**, *15*, 23. (b) Clark, P. W.; Curtis, J. L. S.; Garrou, P. E.; Hartwell, G. E. *Can. J. Chem.* **1974**, *52*, 1714.

(7) (a) Anderson, G. K.; Kumar, R. *Inorg. Chem.* **1984**, *23*, 4064. (b) Saleem, A. M.; Hodali, H. A. *Inorg. Chim. Acta* **1990**, *174*, 223.

However, when **2** was treated with CO (1 atm), facile displacement of the coordinating olefin moiety of the P−olefin ligand by CO took place, giving ($Ph_2PC_2H_4$-$CH{=}CH_2$-κ^1P)(CO)MePt−$MoCp(CO)_3$ (**4**) with a monodentate P−olefin ligand similar to **1**, suggesting the hemilabile nature of the P−olefin ligand (eq 3).

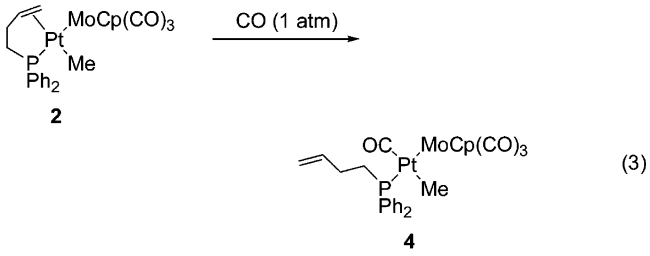

(3)

In contrast, complex **3** did not react at all with CO, suggesting that the P−S ligand is not hemilabile but coordinates strongly to Pt, as observed for a symmetrical bidentate ligand such as *N*,*N*,*N*′,*N*′-tetramethylethylenediamine (TMEDA) or 1,2-bis(diphenylphosphino)ethane (DPPE).[5]

Reactions of Heterodinuclear Methylplatinum−Molybdenum Complexes with Dimethyl Acetylenedicarboxylate. Heterodinuclear organoplatinum−molybdenum complexes having a hemilabile P−N or P−olefin ligand (P−L)MePt−$MoCp(CO)_3$ (P−L = $Ph_2PC_2H_4NEt_2$, (**1**), $Ph_2PC_2H_4CH{=}CH_2$, (**2**)) reacted with dimethyl acetylenedicarboxylate to afford the novel heterodinuclear μ-platinacyclobutenone complexes (P−L)MePt{μ-η^2:η^2-C(O)$C_2(CO_2Me)_2$}$MoCp(\mu$-CO)(CO) (P−L = $Ph_2PC_2H_4NEt_2$ (**5**), $Ph_2PC_2H_4CH{=}CH_2$ (**6**)) (eq 4). In

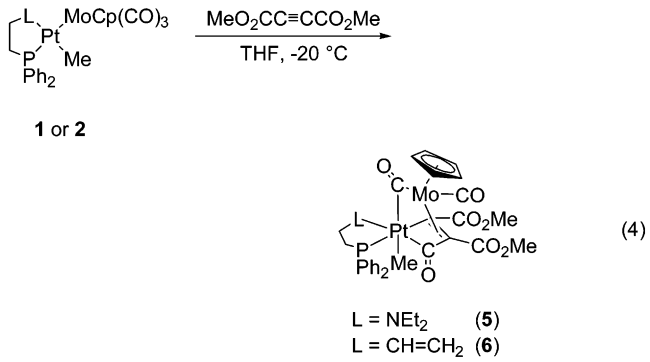

(4)

contrast, complex **3** and analogous heterodinuclear complexes with symmetrical bidentate ligands such as *N*,*N*,*N*′,*N*′-tetramethylethylenediamine (TMEDA) and 1,2-bis(diphenylphosphino)ethane (DPPE), (tmeda)MePt−$MoCp(CO)_3$ and (dppe)MePt−$MoCp(CO)_3$, as well as the mononuclear complex $PtMeCl(Ph_2PC_2H_4NEt_2$-$\kappa^2N,P)$ did not react at all with DMAD under the same reaction conditions. The present high reactivity of **1** and **2** may be attributed to the generation of a vacant coordination site on the platinum center by the facile and partial dissociation of hemilabile P−N or P−olefin ligands, though dynamic behavior due to facile ligand dissociation was not observed in the NMR of **2**. The coordinated DMAD is then considered to couple with bridging CO to give the platinacyclobutenone complexes **5** and **6**.

The molecular structure of complex **5** was established by an X-ray structure analysis. An ORTEP drawing of

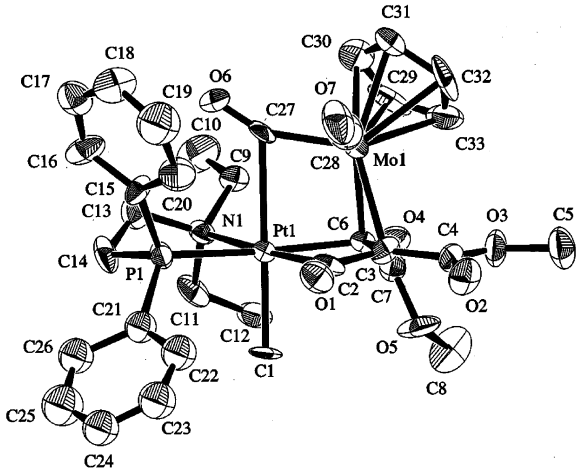

Figure 1. Molecular structure of $(Ph_2PC_2H_4NEt_2$-$\kappa^2N,P)$-MePt$\{\mu$-η^2,η^2-C(O)$C_2(CO_2Me)_2\}$MoCp$(\mu$-CO)(CO) (**5**). All hydrogen atoms are omitted for clarity, and ellipsoids represent 50% probability.

Table 1. Selected Bond Distances (Å) and Angles (deg) for 5

Pt(1)−Mo(1)	2.898(2)	Pt(1)−C(1)	2.21(2)
Pt(1)−P(1)	2.328(5)	Pt(1)−N(1)	2.43(2)
Pt(1)−C(2)	2.09(2)	Pt(1)−C(6)	2.11(2)
Mo(1)−C(3)	2.32(2)	Mo(1)−C(6)	2.11(2)
Mo(1)−C(27)	1.96(2)	Mo(1)−C(28)	2.06(2)
O(1)−C(2)	1.18(2)	O(6)−C(27)	1.18(3)
O(7)−C(28)	1.08(3)	C(2)−C(3)	1.40(3)
C(3)−C(6)	1.45(2)		
Mo(1)−Pt(1)−C(1)	138.5(6)	P(1)−Pt(1)−C(6)	169.8(5)
N(1)−Pt(1)−C(2)	172.2(6)	C(1)−Pt(1)−C(27)	179.7(8)
P(1)−Pt(1)−N(1)	81.6(4)	C(1)−Pt(1)−C(6)	93.6(8)
N(1)−Pt(1)−C(6)	107.1(6)	P(1)−Pt(1)−C(2)	106.1(6)
Mo(1)−C(27)−O(6)	154(1)	Pt(1)−C(27)−O(6)	124(1)
Mo(1)−C(28)−O(7)	178(2)	C(2)−C(3)−C(6)	104(1)
Pt(1)−C(2)−C(3)	96(1)	Pt(1)−C(6)−C(3)	93(1)

5 is depicted in Figure 1, and selected bond distances and angles are given in Table 1. As shown in Figure 1, the geometry around the Pt center is octahedral, suggesting a d^6 electron configuration of Pt(IV). The P−N ligand coordinates as a chelate, and the methyl group is located in the axial position. Furthermore, one of the carbonyl groups attached to Mo is significantly bent (Mo(1)−C(27)−O(6) = 154(1)°) and the C(27) atom is located very close to the Pt center (Pt(1)−C(27) = 2.49(2) Å), suggesting that the bridging carbonyl group C(27)−O(6) occupies one of the coordination sites of Pt. The IR spectrum shows two strong ν(CO) bands in the carbonyl region arising from both terminal (1947 cm^{-1}) and bridging (1779 cm^{-1}) carbonyls.

The C=C double bond of the platinacyclobutenone moiety in **5** also coordinates to Mo to act as a bridging ligand. Analogous unique structures containing π-coordination of metallacyclobutenone to different metals have been known.[8] The two observed Pt−C bond distances of the platinacyclobutenone moiety (Pt(1)−C(2) = 2.09(2) Å, Pt(1)−C(6) = 2.11(2) Å) in **5** are similar to the values of 2.02(3), 2.04(3) Å and 2.08(6), 2.09(4) Å for the known platinacyclobutenone complexes $Pt_2\{\mu$-η^2:η^2-C(Ph)C(Ph)C(O)$\}(\eta$-$C_5H_5)_2$[8a] and $(Ph_3P)_2Pt(OC_3Ph_2)$,[9] respectively. The C=C double-bond distance in the η^2-bonded platinacyclobutenone complex **5** (1.45(2) Å) is comparable to that of $Pt_2\{\mu$-η^2:η^2-C(Ph)C(Ph)C(O)$\}$-$(\eta$-$C_5H_5)_2$ (1.46(4) Å), but it is significantly longer than that of the mononuclear complex $(Ph_3P)_2Pt(OC_3Ph_2)$ (1.31(8) Å). The observed longer C=C double bond is considered to be due to the effective π-back-donation from the Mo metal. Although the Pt−Mo distance 2.898(2) Å in **5** lies in a typical range of Pt−Mo single bonds which have been reported for dinuclear and cluster complexes such as (cod)PhPt−MoCp(CO)$_3$ (2.8320(12) Å),[3b] $(Ph_2C_2H_4NEt_2$-$\kappa^2N,P)$MePt−MoCp(CO)$_3$ (2.8989(9) Å),[5] $Cp_2Mo_2Pt(\mu$-$PPh_2)_2(CO)_5$ (2.860(2), 2.872(2) Å),[10a] and $[(\eta^5$-$C_5H_4Me)Mo(CO)_2(\mu$-dppm)Pt(dppm)$]^+$ (2.912(4) Å),[10b] no actual Pt−Mo interaction is considered to be involved. The Mo moiety in **5** has adopted a three-legged piano-stool type geometry with two carbonyls and one π-bonded platinacyclobutenone ligand. To satisfy the 18-electron rule, we could consider that one electron is transferred from Pt to Mo, making the bond of formally $Pt(IV)^+$ and $Mo(0)^-$ zwitterionic character. However, no significant molar electric conductivity was observed in THF. If the bridging carbonyl is regarded as a one-electron ligand for both metals as if it were a dimetallaketone, formal oxidation states of Pt and Mo are counted as +4 and +2. This formalism is unlikely, because Mo(II) should have a four-legged piano-stool geometry in general, as is typically known for 18e Mo(II) complexes having a Cp group such as CpMo$(CO)_3$Cl.[11] However, this contribution cannot be excluded, since the rare example of Mo(II) complexes having a three-legged structure such as MCl$(CF_3C_2$-$CF_3)_2$Cp (M = Mo, W)[12] is also precedented.

IR spectra of **5** and **6** respectively show strong bands at 1947 and 1960 cm^{-1} assignable to the terminal carbonyl and bands at 1779 and 1774 cm^{-1} due to the bridging carbonyl, consistent with the molecular structure. The ^{1}H NMR spectrum of **5** in acetone-d_6 shows a methyl resonance at δ 0.67 with a ^{195}Pt satellite, two methoxy signals at δ 3.51 and 3.72, and a single Cp resonance at δ 5.40. The NOESY experiment for **5** showed correlation between Cp protons and two methoxy groups of the platinacyclobutenone moiety, consistent with the proximity of these moieties in the geometry of **5**. The $^1J_{Pt-P}$ value of **5** observed in $^{31}P\{^1H\}$ NMR is 2577 Hz, which is significantly smaller than that for **1** (4208 Hz). Analogous trends were also observed for complex **6**. This may be due to the decrease in s character of the Pt−P bond by constructing d^2sp^3

(8) (a) Boag, N. M.; Goodfellow, R. J.; Green, M.; Hessner, B.; Howard, J. A. K.; Stone, F. G. A. *J. Chem. Soc., Dalton Trans.* **1983**, 2585. (b) Chetcuti, M. J.; Green, K. A. *Organometallics* **1988**, *7*, 2450. (c) Finnimore, S. R.; Knox, S. A. R.; Taylor, G. E. *J. Chem. Soc., Chem. Commun.* **1980**, 411. (d) Finnimore, S. R.; Knox, S. A. R.; Taylor, G. E. *J. Chem. Soc., Dalton Trans.* **1982**, 1783. (e) Dickson, R. S.; Evans, G. S.; Fallon, G. D. *Aust. J. Chem.* **1985**, *38*, 273. (f) Chetcuti, M. J.; Eigenbrot, C.; Green, K. A. *Organometallics* **1987**, *6*, 2298. (g) Chetcuti, M. J.; Grant, B. E.; Fanwick, P. E. *Organometallics* **1995**, *14*, 2937. (h) Chetcuti, M. J.; Grant, B. E.; Fanwick, P. E. *Organometallics* **1996**, *15*, 4389.

(9) Jones, R. A. Y.; Katritzky, A. R.; Richards, A. C.; Saba, S.; Sparrow, A. J.; Trepanier, D. L. *J. Chem. Soc., Chem. Commun.* **1972**, 673.

(10) (a) Blum, T.; Braunstein, P. *Organometallics* **1989**, *8*, 2504. (b) Braunstein, P.; Bellefon, C. M.; Lanfranchi, M.; Tiripicchino, A. *Organometallics* **1984**, *3*, 1772.

(11) (a) Bueno, C.; Churchill, M. R. *Inorg. Chem* **1981**, *20*, 2197. (b) Poli, R. *Organometallics* **1990**, *9*, 1892.

(12) (a) Davidson, J. L.; Green, M.; Sharp, D. W. A.; Stone, F. G. A.; Welch, A. J. *J. Chem. Soc., Chem. Commun.* **1974**, 706. (b) Davidson, J. L.; Green, M.; Stone, F. G. A.; Welch, A. J. *J. Chem. Soc., Dalton Trans.* **1976**, 738. (c) Davidson, J. L.; Green, M.; Nyathi, J. Z.; Stone, F. G. A.; Welch, A. J. *J. Chem. Soc., Dalton Trans.* **1977**, 2246.

hybridization of octahedral Pt(IV) for **5** and **6** in comparison with dsp^2 hybridization for the square-planar Pt(II) complex **1**. The trans influence of sp^2-C instead of Mo and the high oxidation state of Pt in **5** and **6** are also considered to decrease the coupling constant.

Complex **1** also reacted with diethyl acetylenedicarboxylate to form the μ-platinacyclobutenone complex ($Ph_2PC_2H_4NEt_2$-κ^2N,P)MePt{μ-η^2:η^2-C(O)C_2(CO_2Et)$_2$}MoCp(μ-CO)(CO) (**7**), but other alkynes such as diphenylacetylene, 1-phenyl-1-propyne, and ethyl 2-butynoate did not react with **1** under the same reaction conditions. This result suggests the importance of highly electron-withdrawing substituents on acetylene for the reaction to proceed.

Thermal Transformation of Platinacyclobutenone to an Alkenylplatinum−Molybdenum Dinuclear Complex. Heating of the platinacyclobutenone complex **5** at 50 °C in acetone-d_6 for 2 days caused apparent insertion of DMAD into the Pt−Me bond to form a mixture of the new μ-alkenyl type complexes ($Ph_2PC_2H_4NEt_2$-κ^2N,P){μ-$MeO_2C(Me)$=CCO_2Me}Pt−MoCp(μ-CO)(CO) (**8**) and ($Ph_2PC_2H_4NEt_2$-κ^1P)(CO){μ-$MeO_2C(Me)$=CCO_2Me}Pt−MoCp(μ-CO)(CO) (**9**), in the latter of which the coordinating nitrogen atom in **8** was displaced by CO (eq 5). The rare complex **8** was isolated

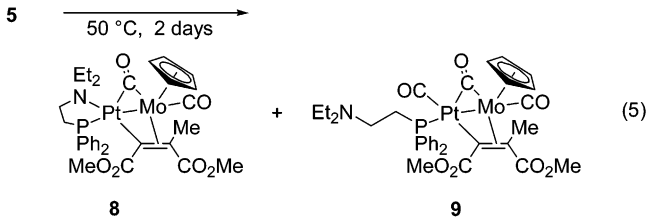

(5)

from the mixture by recrystallization from acetone/hexane. The reaction is considered to proceed by initial formation of **8** followed by coordination of the liberated CO, since the ratio of **8** to **9** gradually decreased during the reaction. In fact, the treatment of the isolated **8** with 1 atm of CO immediately gave **9** at room temperature. On the other hand, when **9** was heated at 50 °C in acetone-d_6 under reduced pressure, complex **8** was slowly regenerated. Decrease in the ratio of **8** to **9** in the course of the reaction may indicate that initial decarbonylation in **5** gives **8** by reductive elimination, followed by coordination of CO. The result also suggests that **5** is the kinetic product but μ-alkenyl type complexes **8** and **9** are the thermodynamic products in the reaction of **1** with DMAD.

The failure of the direct insertion in the reaction of **1** with DMAD may be due to the resultant trans geometry of Me and DMAD in the initial stage of the reaction, and thus the coupling of DMAD and bridging CO became a favorable reaction pathway instead.

Single crystals of **8** suitable for X-ray structure analysis were fortunately obtained by recrystallization from acetone/hexane. Selected bond distances and angles are summarized in Table 2, and an ORTEP drawing is depicted in Figure 2. The alkenyl group on Pt coordinates to the Mo center via the C=C double bond (C(19)−C(22) = 1.43(1) Å, Mo(1)−C(19) = 2.155(7) Å, Mo(1)−C(22) = 2.341(7) Å), and one of the carbonyls acts as a bridging ligand (Pt(1)−C(26) = 2.487(8) Å, Mo(1)−C(26) = 1.949(8) Å). The bridging carbonyl in **8** is bent (Mo(1)−C(26)−O(5) = 160.5(7)°, Pt(1)−C(26)−O(5) = 120.8(6)°), suggesting strong bridging character in **8**. The Pt−Mo bond distance of **8** is 2.8302(7) Å, which is slightly shorter than that of complex **5**. The geometry at the Pt center is considered to be square planar with a P−N ligand, alkenyl, and Mo−CO moieties, where the least-squares plane consisting of Pt(1), P(1), N(1), C(19), and the central position of Mo(1)−C(26) has a largest deviation of only 0.14 Å from the plane. Mo and the carbonyl carbon C(26) deviate 0.47 Å from this plane. One possible formalism of the bonding scheme is the side-on type coordination of the Mo−CO bond to Pt, and the apparent oxidation states of Pt and Mo in **8** are considered to be +2 and 0, giving again a Pt^+ and Mo^- zwitterionic structure. However, contribution to the coordination by a canonical Mo=C=O double bond structure is not the case, since the CO stretching band is similar to other cases, but the Mo−CO single bond interacts with Pt. A five-coordinate tbp structure formalism of the Pt center having a chelating P−N ligand, alkenyl carbon, Mo, and bridging carbonyl may also be possible, with the N(1) and C(19) atoms in apical positions, because the Pt(1), P(1), N(1), and C(19) atoms constitute an almost complete plane. An analogous structural feature was also observed for the independently prepared complex (dppe)(μ-CH_2=CCO_2Me)Pt−MoCp(μ-CO)(CO), obtained by the reaction of (dppe)(H)Pt−MoCp$(CO)_3$ with HC≡CCO_2Me.[3f] It is interesting to note that the difference of oxidation states in **5** and

Table 2. Selected Bond Distances (Å) and Angles (deg) for 8

Pt(1)−Mo(1)	2.8302(7)	Pt(1)−N(1)	2.244(6)
Pt(1)−P(1)	2.251(2)	Pt(1)−C(19)	2.021(7)
Pt(1)−C(26)	2.487(8)	Mo(1)−C(19)	2.155(7)
Mo(1)−C(22)	2.341(7)	Mo(1)−C(26)	1.949(8)
Mo(1)−C(27)	1.951(8)	C(19)−C(22)	1.43(1)
C(26)−O(5)	1.168(10)	C(26)−O(6)	1.16(1)
Mo(1)−Pt(1)−P(1)	151.46(5)	Mo(1)−Pt(1)−N(1)	124.0(2)
Mo(1)−Pt(1)−C(19)	49.4(2)	Mo(1)−Pt(1)−C(26)	42.4(2)
P(1)−Pt(1)−N(1)	83.3(2)	P(1)−Pt(1)−C(19)	103.1(2)
P(1)−Pt(1)−C(26)	164.1(2)	N(1)−Pt(1)−C(19)	173.2(3)
N(1)−Pt(1)−C(26)	86.8(3)	C(19)−Pt(1)−C(26)	87.5(3)
Pt(1)−C(26)−O(5)	120.8(6)	Mo(1)−C(26)−O(5)	160.5(7)
Mo(1)−C(27)−O(6)	179.1(8)		

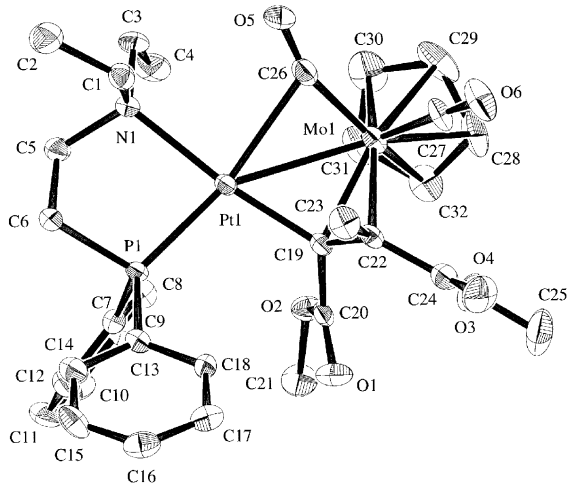

Figure 2. Molecular structure of ($Ph_2PC_2H_4NEt_2$-κ^2N,P)-{μ-$MeO_2C(Me)C$=CCO_2Me}Pt−MoCp(μ-CO)(CO) (**8**). All hydrogen atoms are omitted for clarity, and ellipsoids represent 50% probability.

8 is reflected in their CO stretching bands, where the values for **5** are larger than those for **8** by ca. 30 cm^{-1}, being consistent with stronger back-donation in Pt(II) than in Pt(IV), although the slight structural difference of the Mo moiety may interfere with such a discussion. The coupling constant $^1J_{Pt-P}$ for **8** in the $^{31}P\{^1H\}$ NMR spectrum is significantly large (4010 Hz). This also suggests an increase in s-character of the Pt−P bond in **8** over that in **5**.

Complex **9** was also characterized by NMR. The chemical shift of the signals due to the diethylamino moiety of the P−N ligand were almost the same as those for free 2-(diphenylphosphino)triethylamine in ^1H NMR, suggesting the ligand displacement of an N atom by CO. The $^{31}P\{^1H\}$ NMR spectrum showed a singlet with a ^{195}Pt satellite ($^1J_{Pt-P}$ = 3136 Hz). The small $^1J_{Pt-P}$ value of **9** may be due to the decrease of electron density at Pt by the coordination of CO, and a similar trend was observed for complex **4**.

The present reaction is considered to proceed by a mechanism involving cis reductive elimination of alkenyl and methyl ligands at Pt(IV) followed by decarbonylation to give a formal insertion of DMAD into the Pt−Me bond. Initial decarbonylation providing a cis geometry of DMAD and methyl ligands followed by facile cis insertion is another possible mechanism.

Ligand Displacement Reaction of 5 with ^{t}BuNC and PMe_3. The μ-platinacyclobutenone complex **5** displaced the hemilabile N atom in the P−N ligand by ^{t}BuNC or PMe_3 to give corresponding complexes with a monodentate P−N ligand, $(Ph_2PC_2H_4NEt_2\text{-}\kappa^1P)$(L′)MePt{$\mu$-$\eta^2$:$\eta^2$-C(O)$C_2$($CO_2$Me)$_2$}MoCp($\mu$-CO)(CO) (L′ = ^{t}BuNC (**10**), PMe_3 (**11**)) (eq 6). Complex **10** was isolated as

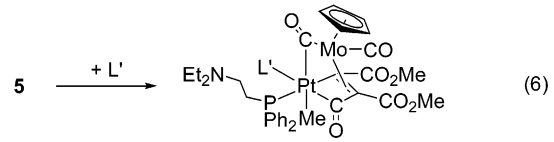

(6)

L' = ^{t}BuNC (**10**), PMe_3 (**11**)

orange crystals by recrystallization from a mixture of acetone and hexane in the presence of an excess amount of ^{t}BuNC. In the absence of an excess amount of ^{t}BuNC, **10** dissociated ^{t}BuNC to regenerate **5**.

The structure of **10** was confirmed by an X-ray diffraction study (Figure 3, Table 3). There are no significant differences in the geometry around Pt and Mo in comparison with complex **5**. The P−N ligand acts as a monodentate ligand in **10**, and ^{t}BuNC was coordinated to the Pt center instead of the diethylamino moiety. The terminal isonitrile ligand exhibits approximately linear geometry (C(20)−N(2)−C(21) = 175(1)°). The Pt(1)−C(20) and N(2)−C(20) distances (2.095(7) and 1.12(1) Å, respectively) are close to the values found in [Pt_3(μ-dppm)$_2$(μ-PPh_2)(^{t}BuNC)]OTf (mean Pt−C = 1.96 Å and mean C−N = 1.15 Å)[13a] and [(C−N−N)Pt(^{t}BuNC)]ClO_4 (C−N−N = 6-phenyl-2,2′-bipyridine; Pt−C = 1.936(8) Å and C−N = 1.13(1) Å).[13b]

In the ^1H NMR spectrum of **10**, the methylene signals of the −NC$H_2$$CH_3$ moiety shifts upfield compared with

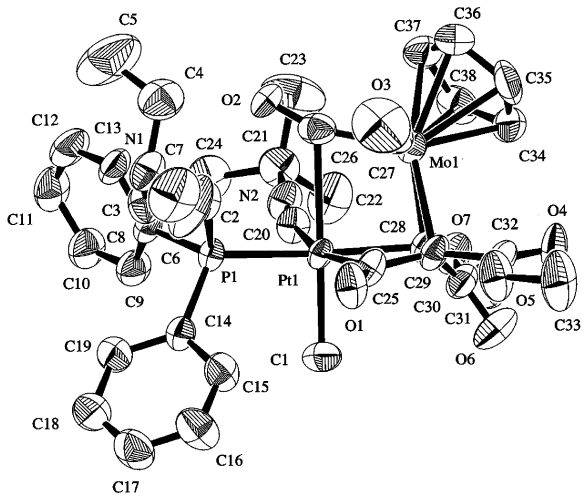

Figure 3. Molecular structure of $(Ph_2PC_2H_4NEt_2\text{-}\kappa^1P)$(^{t}BuNC)MePt{$\mu$-$\eta^2$,$\eta^2$-C(O)$C_2$($CO_2$Me)$_2$}MoCp($\mu$-CO)(CO) (**10**). All hydrogen atoms are omitted for clarity, and ellipsoids represent 50% probability.

Table 3. Selected Bond Distances (Å) and Angles (deg) for 10

Pt(1)−Mo(1)	2.875(1)	Pt(1)−C(1)	2.352(4)
Pt(1)−C(1)	2.129(9)	Pt(1)−C(20)	2.095(7)
Pt(1)−C(25)	2.080(7)	Pt(1)−C(26)	2.526(9)
Pt(1)−C(28)	2.104(9)	Mo(1)−C(26)	1.96(1)
Mo(1)−C(27)	2.00(1)	Mo(1)−C(28)	2.124(9)
Mo(1)−C(29)	2.303(8)	O(1)−C(25)	1.204(10)
O(2)−C(26)	1.18(1)	O(3)−C(27)	1.16(1)
N(2)−C(20)	1.12(1)	N(2)−C(21)	1.45(1)
C(25)−C(29)	1.42(1)	C(28)−C(29)	1.44(1)
Mo(1)−Pt(1)−C(1)	139.3(3)	P(1)−Pt(1)−C(28)	162.7(2)
C(1)−Pt(1)−C(26)	172.9(3)	C(20)−Pt(1)−C(25)	164.3(3)
P(1)−Pt(1)−C(20)	95.9(2)	C(20)−Pt(1)−C(28)	99.4(3)
P(1)−Pt(1)−C(25)	97.6(2)	C(25)−Pt(1)−C(28)	66.2(3)
Pt(1)−C(20)−N(2)	168.6(8)	C(20)−N(2)−C(21)	175(1)
Pt(1)−C(26)−O(2)	119.2(8)	Mo(1)−C(28)−O(2)	161.9(8)
Mo(1)−C(27)−O(3)	177(1)	Pt(1)−C(25)−C(29)	94.3(5)
Pt(1)−C(28)−C(29)	92.9(5)	C(25)−C(29)−C(28)	105.9(7)

the signals for **5** and are almost similar to those of free 2-(diphenylphosphino)triethylamine. The $^{31}P\{^1H\}$ NMR spectrum shows a single resonance at δ −12.1 with a ^{195}Pt satellite ($^1J_{Pt-P}$ = 2348 Hz). A further decrease in $^1J_{Pt-P}$ value in comparison with **5** is the reflection of effective back-donation to the isonitrile ligand to decrease the electron density at Pt.

Complex **11** was characterized spectroscopically by NMR and IR. In the ^1H NMR spectrum, the chemical shift of the methylene group of −NC$H_2$$CH_3$ was close to that of free $Ph_2PC_2H_4NEt_2$. The Pt−Me group appears as a double doublet at δ 0.70 with a ^{195}Pt satellite, indicating two magnetically inequivalent phosphorus nuclei attached to Pt. Consistently, $^{31}P\{^1H\}$ NMR shows two doublets with a small cis coupling constant ($^2J_{P-P}$ = 13 Hz) having ^{195}Pt satellites. The IR spectrum of **11** also shows ν(CO) bands similar to those of **5** and **10**.

Reaction of 5 with Nucleophiles. The acyl group of **5** attached to an electron-deficient Pt(IV) center was susceptible to nucleophilic reactions. In fact, H_2NBu, $HNEt_2$, or pyrrolidine readily attacked the Pt−acyl carbon of the platinacyclobutenone moiety, to give a novel hetereodinuclear complex having a bridging trisubstituted alkenyl group, $(Ph_2PC_2H_4NEt_2\text{-}\kappa^2N,P)$Me{$\mu$-Me$O_2$C($R_2$NCO)C=CC$O_2$Me}Pt−MoCp($\mu$-CO)(CO) ($NR_2$ =

(13) (a) Wachtler, H.; Schuh, W.; Ongania, K.; Wurst, K.; Peringer, P. *Organometallics* **1998**, *17*, 5649. (b) Lai, S.; Lam, H.; Lu, W.; Cheung, K.; Che, C. *Organometallics* **2002**, *21*, 226.

Scheme 2

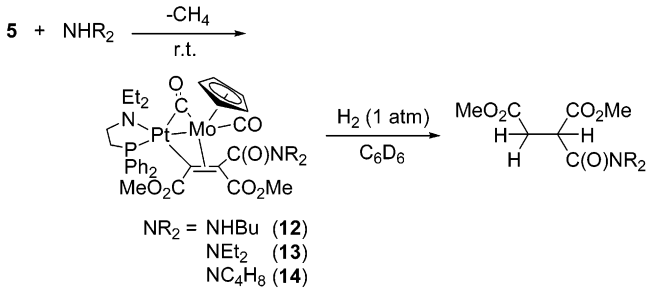

NHBu (**12**), NEt_2 (**13**), NC_4H_8 (**14**)) with evolution of methane (Scheme 2). In contrast to these results, sterically demanding secondary amines such as HN^iPr_2 and $HNPh_2$ and a tertiary amine such as NEt_3 did not react at all with **5**. This may be attributed to the steric congestion at Pt in **5** to prevent attack of these amines. The reaction is considered to proceed by initial nucleophilic reaction of dialkyl amide anion with the acyl carbon, followed by reductive elimination of methane. It is not clear whether a hydridoplatinum(IV) species is formed or not as an intermediate prior to the reaction.

In the IR spectrum of **13**, two ν(CO) bands arising from bridging and terminal carbonyls on Mo appeared at 1715 and 1958 cm^{-1} and a new band due to the resulting amide moiety was also observed at 1618 cm^{-1}. In the $^{31}P\{^1H\}$ NMR spectrum, a singlet with a ^{195}Pt satellite having the large $^1J_{Pt-P}$ value of 4298 Hz was observed, similarly to μ-alkenyl complex **8** ($^1J_{Pt-P}$ = 4010 Hz). In the ^1H NMR spectrum of **13**, two methyl groups of the diethylamide moiety were inequivalent, showing two broad signals at δ 1.06 and 1.13. In addition, the corresponding methylene resonances of the diethylamide group were observed as diastereotopic (3.3−3.6 (3H, br) and 3.95 (1H, br)). These results indicate the restricted rotation of the N−C(O) bond due to the significant contribution of carbon−nitrogen double-bond character[14] and the diastereotopic nature of methylene protons by the π-coordination of the C=C bond to the Mo center. From these observations, the analogous structure of **13** is proposed as depicted in Scheme 2.

Treatments of **13** and **14** with 1 atm of hydrogen gas at ambient temperature resulted in the hydrogenation and hydrogenolysis of the Pt−alkenyl moiety, giving dialkylcarbamoyl dimethylsuccinate, though unfortunately the inorganic products could not be characterized due to their extensive reduction to metal (Scheme 2). This fact also supports the proposed structure of these complexes.

KOPh also reacted with **5** to give a new ate complex having a μ-alkenyl group, $K^+[(Ph_2PC_2H_4NEt_2\text{-}\kappa^1P)Me\{\mu\text{-}MeO_2C(PhO_2C)C{=}CCO_2Me\}Pt{-}MoCp(\mu\text{-}CO)(CO)]^-$ (**15**) (eq 7).

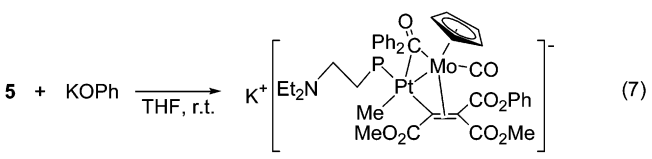

15

(14) Gutowsky, H. S.; Holm, C. H. *J. Chem. Phys.* **1956**, *25*, 1228.

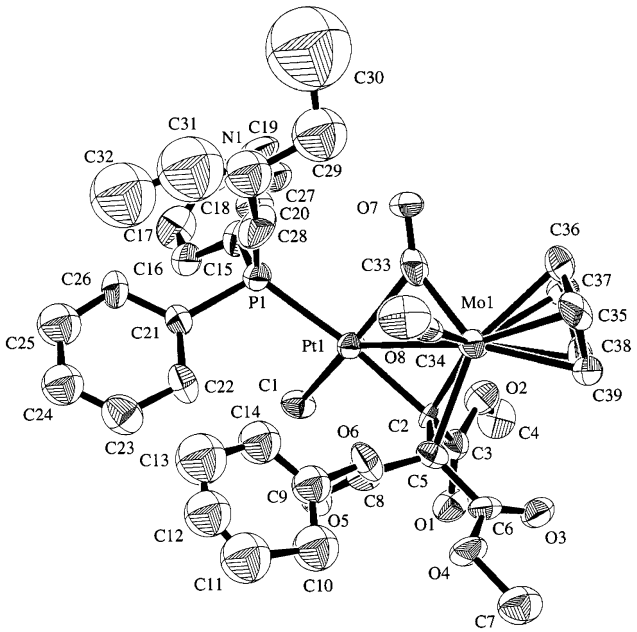

Figure 4. Molecular structure of $K^+[(Ph_2PC_2H_4NEt_2\text{-}\kappa^1P)Me\{\mu\text{-}MeO_2C(PhO_2C)C{=}CCO_2Me\}Pt{-}MoCp(\mu\text{-}CO)(CO)]^-$ (**15**). All hydrogen atoms, the solvent molecule, and K^+ moiety are omitted for clarity, and ellipsoids represent 30% probability.

The structure of **15** was characterized spectroscopically as well as by preliminary X-ray structure analysis. In the IR spectrum, a new ν(C=O) band of the resulting CO_2Ph group was observed at 1592 cm^{-1}, in addition to the large bands due to terminal and bridging carbonyls and CO_2Me groups. The methylene protons of the ethyl group were observed to be very close to those of the free P−N ligand, similarly to **9**−**11** in the ^1H NMR, suggesting partial dissociation of the diethylamino group to behave as a monodentate ligand. A preliminary X-ray structure analysis supported a square-planar geometry of **15** similar to that of **8**, as depicted in Figure 4. The bridging carbonyl carbon deviates by 0.78(3) Å from the least-squares plane consisting of P, Me, alkenyl, and Mo (maximum deviation 0.21(2) Å). The relatively small $^1J_{Pt-P}$ value for **15** (3038 Hz) in the $^{31}P\{^1H\}$ NMR compared with those of **8** and **12**−**14** may reflect the stronger trans influence of alkenyl carbon as compared to that of bridging carbonyl.

Reaction of **15** with methyl iodide gave the dimethyl(alkenyl)(P−N ligand)platinum−molybdenum complex $(Ph_2PC_2H_4NEt_2\text{-}\kappa^2N,P)Me_2\{\mu\text{-}MeO_2C(PhO_2C)C{=}CCO_2Me\}Pt{-}MoCp(\mu\text{-}CO)(CO)$ (**16**), where two methyl ligands are inequivalent, indicating that they are cis to each other. Although the detailed structure of **16** is not clear at present, the P−N ligand is considered to coordinate in a bidentate fashon. Again the $^1J_{Pt-P}$ value (2105 Hz) is small, suggesting Pt(IV) and Mo(0) as discussed before. The IR spectrum of **16** shows two strong ν(CO) bands in the carbonyl region arising from both terminal (1925 cm^{-1}) and bridging (1744 cm^{-1}) carbonyls, respectively, suggesting a six-coordinated structure containing a bridging carbonyl group, as depicted in Scheme 3.

On the other hand, protonolysis of **15** with HCl/acetone did not afford trisubstituted olefin, but the μ-alkenyl type complex $(Ph_2PC_2H_4NEt_2\text{-}\kappa^2N,P)\{\mu\text{-}MeO_2C(PhO_2C)C{=}CCO_2Me\}Pt{-}MoCp(\mu\text{-}CO)(CO)$ (**17**) was

Scheme 3

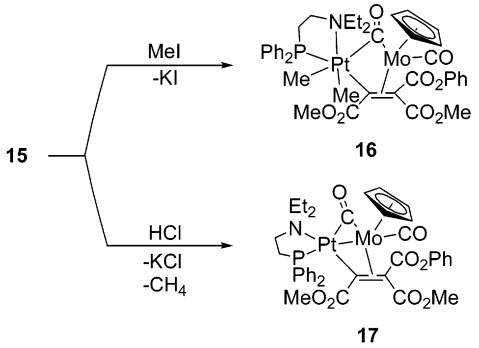

formed with liberation of methane. The $^{31}P\{^1H\}$ NMR of **17** showed a single resonance with a ^{195}Pt satellite, which has a large $^1J_{Pt-P}$ value (4139 Hz) similar to that of the (μ-alkenyl)platinum(II) complex **8** mentioned above. In the ^1H NMR, all resonances for the coordinating P−N ligand, alkenyl group, and Cp group on Mo were also observed, and their chemical shifts are similar to those of **8**. These results suggest that **17** has the μ-alkenyl structure depicted in Scheme 3.

Concluding Remarks

In the present study, we have synthesized novel Pt−Mo heterodinuclear organometallic complexes having an unsymmetrical P−olefin or P−S ligand. Heterodinuclear complexes with hemilabile ligands, **1** and **2**, show higher reactivity toward DMAD than do **3** and analogous complexes with symmetrical bidentate ligands such as TMEDA and DPPE, to give new metallacyclobutenone complexes. Facile generation of a reactive vacant coordination site on the Pt center caused by the hemilabile character of the ligand and cooperative effects of the two metals are considered to play crucial roles in the process of coupling of CO and DMAD and the formal insertion process, though the mechanistic details are not clear at present.

Although further functionalizations of these alkenyl ligands by demetalation in these heterodinuclear systems were unsuccessful, the present selective reactions of Pt−Mo heterodinuclear complexes with hemilabile P−N ligands are of great interest in connection with the possible catalytic functionalization of alkynes by bimetallic catalysts.

Experimental Section

All manipulations were carried out under a dry nitrogen or argon atmosphere using standard Schlenk and vacuum-line techniques. Solvents were refluxed over and distilled from appropriate drying agents under N_2: benzene, toluene, hexane, THF, and Et_2O from sodium benzophenone ketyl; acetone from Drierite; CH_2Cl_2 from P_2O_5. Deuterated solvents were degassed by three freeze−pump−thaw cycles and then vacuum transferred from appropriate drying agents (C_6D_6 from sodium wire, CD_3COCD_3 from Drierite). NMR spectra were recorded on a JEOL LA-300 spectrometer (300.4 MHz for ^1H, 121.6 MHz for ^{31}P) with chemical shifts reported in ppm downfield from TMS for ^1H and from 85% H_3PO_4 in D_2O. Product yields for reactions in a NMR tube were calculated on the basis of internal $CHPh_3$. IR spectra were recorded on a JASCO FT/IR-410 spectrometer using KBr disks. Elemental analyses were carried out with a Perkin-Elmer 2400 Series II CHN analyzer. The molar electrical conductivity was measured on a TOA CM 7B Conduct Meter. GC-MS analysis was performed on a Shimadzu GCMS-QP2000A using a GL Science 30 m × 0.25 mm TC-WAX capillary column.

($Ph_2PC_2H_4CH{=}CH_2$-κ^2*P,olefin*)MePt−MoCp(CO)$_3$ (2). (cod)MePt−$MoCp(CO)_3$ (166.9 mg, 0.2963 mmol) was placed in a Schlenk tube under nitrogen, and benzene was added. Then $Ph_2PC_2H_4CH{=}CH_2$ (70 μL, 0.28 mmol) was added and stirred at room temperature for 1 day. After the solution was concentrated under reduced pressure, excess hexane was added to give an analytically pure yellow powder. Yield: 81% (181.7 mg, 0.2399 mmol). Anal. Calcd for $C_{25}H_{25}MoO_3PPt$: C, 43.18; H, 3.62. Found: C, 42.92; H, 3.55. ^1H NMR (C_6D_6): δ 1.30 (3H, d, $^3J_{P-H}$ = 5.7 Hz, $^2J_{Pt-H}$ = 77 Hz, Pt−Me), 1.6−1.9 (4H, m, CH_2CH_2), 3.89 (1H, d, $^3J_{H-H}$ = 17.7 Hz, $^2J_{Pt-H}$ = 32.4 Hz, CH=CH_2), 4.83 (1H, d, $^3J_{H-H}$ = 9.3 Hz, $^2J_{Pt-H}$ = 35.1 Hz, CH=CH_2), 5.08 (5H, s, Cp), 5.41 (1H, m, CH=CH_2), 7.01−7.03 (6H, m, *m*- and *p*-Ph), 7.53−7.60 (4H, m, *o*-Ph). $^{31}P\{^1H\}$ NMR (C_6D_6): δ 42.0 (s, $^1J_{Pt-P}$ = 3584 Hz). IR (KBr, cm^{-1}): 1795 (vs), 1904 (vs).

($Ph_2PC_2H_4SMe$-κ^2*P,S*)MePt−MoCp(CO)$_3$ (3). PtMeCl($Ph_2PC_2H_4SMe$-κ^2*P,S*) (121.9 mg, 0.2296 mmol) and $AgNO_3$ (63.6 mg, 0.374 mmol) were dissolved in THF, and the suspension was stirred overnight at room temperature to give a pale yellow solution with a white precipitate of AgCl. The precipitate was filtered off, and the resulting solution was added dropwise to a THF solution of Na[$MoCp(CO)_3$][15] (88.4 mg, 0.329 mmol) under −70 °C and the mixture was stirred for 3 h at −30 °C. All volatile matter was removed by evaporation, and the resulting brown-yellow solid was extracted with toluene at −20 °C. After the filtered solution was concentrated under reduced pressure at −20 °C, excess hexane was added to give an analytically pure yellow powder. The product was filtered, washed with hexane, and dried under vacuum at room temperature. Yield: 70% (115.2 mg, 0.1610 mmol). Anal. Calcd for $C_{24}H_{25}MoO_3PPtS$: C, 40.29; H, 3.52; S, 4.48. Found: C, 40.68; H, 3.64; S, 4.59. ^1H NMR (CD_3COCD_3): δ 0.55 (3H, d, $^3J_{P-H}$ = 5.7 Hz, $^2J_{Pt-H}$ = 73.9 Hz, Pt−Me), 2.5−3.3 (4H, br, CH_2CH_2), 2.56 (3H, s, $^3J_{Pt-H}$ = 19.5 Hz, SMe), 5.32 (5H, s, Cp), 7.5−7.8 (10H, m, Ph). $^{31}P\{^1H\}$ NMR (CD_3COCD_3): δ 57.4 (s, $^1J_{Pt-P}$ = 3734 Hz). IR (KBr, cm^{-1}): 1791 (vs), 1897 (vs).

($Ph_2PC_2H_4CH{=}CH_2$-κ^1*P*)(CO)MePt−MoCp(CO)$_3$ (4). 2 (71.0 mg, 0.104 mmol) was dissolved in toluene, and the solution was degassed. Carbon monoxide (1 atm) was then introduced. After the mixture was stirred for 2 h at ambient temperature, a large amount of hexane (ca. 20 mL) was added to the solution, and then the yellow solution was filtered and cooled to −30 °C to give pale yellow crystals of **4**. Yield: 98% (74.0 mg, 0.102 mmol). Anal. Calcd for $C_{26}H_{25}MoO_4PPt\cdot 0.5C_7H_8$: C, 46.04; H, 3.80. Found: C, 46.18; H, 3.96. ^1H NMR (CD_3COCD_3): δ 0.71 (3H, d, $^3J_{P-H}$ = 8.4 Hz, $^2J_{Pt-H}$ = 61.8 Hz, Pt−Me), 2.50 (2H, m, CH_2CH_2), 2.93 (2H, m, CH_2CH_2), 5.01 (1H, brd, $^3J_{H-H}$ = 10.0 Hz, CH=CH_2), 5.14 (1H, dq, $^3J_{H-H}$ = 17.1 Hz, $^2J_{H-H}$ = $^4J_{H-H}$ = 1.5 Hz, CH=CH_2), 5.43 (5H, s, Cp), 5.96 (1H, ddt, $^3J_{H-H}$ = 17.1, 10.0, 6.3 Hz, CH=CH_2), 7.54−7.58 (6H, m, *m*- and *p*-Ph), 7.72−7.80 (4H, m, *o*-Ph). $^{31}P\{^1H\}$ NMR (CD_3COCD_3): δ 29.4 (s, $^1J_{Pt-P}$ = 2965 Hz). IR (KBr, cm^{-1}): 1832 (vs), 1921 (vs), 2050 (s).

($Ph_2PC_2H_4NEt_2$-κ^2*N,P*)MePt{μ-η^2:η^2-C(O)C_2(CO_2Me)$_2$}-MoCp(μ-CO)(CO) (5). Dimethyl acetylenedicarboxylate (DMAD; 20 μL, 0.16 mmol) was added to a solution of the complex ($Et_2NC_2H_4PPh_2$-κ^2*N,P*)MePt−$MoCp(CO)_3$ (**1**; 135 mg, 0.153 mmol) in acetone at −30 °C, and the reaction mixture was stirred for 12 h at −30 °C. Then, the solution was concentrated under reduced pressure at room temperature, and excess hexane was added to give an analytically pure yellow powder. Yield: 71% (97 mg, 0.11 mmol). Anal. Calcd for $C_{33}H_{38}MoNO_7PPt$: C, 44.90; H, 4.34; N, 1.59. Found: C, 44.44; H, 4.53; N, 1.60. Molar electrical conductivity Λ (THF, 20 °C): 0.0012 S

(15) Piper, T. S.; Wilkinson, G. *J. Inorg. Nucl. Chem*. **1956**, *3*, 104.

$cm^2\ mol^{-1}$. ^1H NMR (CD_3COCD_3): δ 0.67 (3H, d, $^3J_{P-H} = 6.9$ Hz, $^2J_{Pt-H} = 76.6$ Hz, Pt−Me), 0.92 (6H, t, $^3J_{H-H} = 7.5$ Hz, Me (NEt)), 2.5−3.2 (8H, m, CH_2 (NEt) and CH_2CH_2), 3.51 (3H, s, OMe), 3.72 (3H, s, OMe), 5.40 (5H, s, Cp), 7.3−7.4 (6H, m, *m*- and *p*-Ph), 7.7−7.9 (4H, m, *o*-Ph). $^{31}P\{^1H\}$ NMR (CD_3COCD_3): δ 7.2 (s, $^1J_{Pt-P} = 2577$ Hz). IR (KBr, cm^{-1}): 1691 (vs), 1706 (vs), 1779 (vs), 1947 (vs).

($Ph_2PC_2H_4CH{=}CH_2$-κ^2*P,olefin*)MePt{μ-η^2:η^2-C(O)C_2(CO_2Me)$_2$}MoCp(μ-CO)(CO) (6). Dimethyl acetylenedicarboxylate (DMAD; 12 μL, 0.098 mmol) was added to a solution of the complex ($Ph_2PC_2H_4CH{=}CH_2$-κ^2*P,olefin*)MePt−MoCp(CO)$_3$ (**2**; 62.8 mg, 0.0922 mmol) in acetone at −30 °C and the reaction mixture was stirred for 12 h at −30 °C. Then, the solution was concentrated under reduced pressure at −30 °C, and excess hexane was added to give an analytically pure yellow powder. Yield: 65% (50.2 mg, 0.0599 mmol). Anal. Calcd for $C_{31}H_{31}MoO_7PPt$: C, 44.45; H, 3.37. Found: C, 44.89; H, 3.95. ^1H NMR (CD_3COCD_3): δ 0.58 (3H, d, $^3J_{P-H} = 6.9$ Hz, $^2J_{Pt-H} = 75.3$ Hz, Pt−Me), 2.0−3.0 (4H, m, CH_2CH_2), 3.52 (3H, s, OMe), 3.76 (3H, s, OMe), 4.60 (1H, m, CH=CH_2), 4.93 (1H, m, CH=CH_2), 5.49 (5H, s, Cp), 5.76 (1H, m, C*H*=CH_2), 7.3−7.7 (10H, m, Ph). $^{31}P\{^1H\}$ NMR (CD_3COCD_3): δ 10.5 (s, $^1J_{Pt-P} = 2639$ Hz). IR (KBr, cm^{-1}): 1678 (s), 1702 (s), 1725 (vs), 1774 (vs), 1960 (s).

($Ph_2PC_2H_4NEt_2$-κ^2*N,P*)MePt{μ-η^2:η^2-C(O)C_2(CO_2Et)$_2$}-MoCp(μ-CO)(CO) (7). Diethyl acetylenedicarboxylate (14 μL, 0.088 mmol) was added to a solution of the complex **1** (55.2 mg, 0.0745 mmol) in toluene at −30 °C, and the reaction mixture was stirred for 4 h at −30 °C. After removal of all volatile matters under vacuum, the resulting orange solid was washed with hexane and recrystallized from THF/hexane to give orange crystals. Yield: 71% (56.9 mg, 0.0624 mmol). ^1H NMR (CD_3COCD_3): δ 0.68 (3H, d, $^3J_{P-H} = 6.6$ Hz, Pt−Me), 0.93 (6H, t, $^3J_{H-H} = 6.9$ Hz, Me (NEt)), 1.18 (3H, t, $^3J_{H-H} = 6.9$ Hz, Me (OEt)), 1.29 (3H, t, $^3J_{H-H} = 6.9$ Hz, Me (OEt)), 2.7−3.2 (8H, br, CH_2 (NEt) and CH_2CH_2), 3.88−4.31 (4H, m, CH_2 (OEt)), 5.41 (5H, s, Cp), 7.32−7.38 (6H, m, *m*- and *p*-Ph), 7.76−7.91 (4H, m, *o*-Ph). $^{31}P\{^1H\}$ NMR (CD_3COCD_3): δ 7.4 (s, $^1J_{Pt-P} = 2578$ Hz). IR (KBr, cm^{-1}): 1678 (s), 1712 (s), 1790 (s), 1951 (vs).

($Ph_2PC_2H_4NEt_2$-κ^2*N,P*){μ-MeO_2C(Me)C=CCO_2Me}Pt−MoCp(μ-CO)(CO) (8). Complex **5** (43 mg, 0.049 mmol) was dissolved in acetone, and the solution was heated at 50 °C for 2 days. The solution turned from yellow to red-orange. The solution was evaporated under reduced pressure and recrystallized from acetone/hexane to give yellow crystals. Yield: 31% (15 mg, 0.015 mmol). Anal. Calcd for $C_{32}H_{38}MoNO_6PPt$: C, 44.97; H, 4.48; N, 1.64. Found: C, 45.28; H, 4.41; N, 1.66. Molar electrical conductivity Λ (THF, 24 °C): 0.069 S $cm^2\ mol^{-1}$. ^1H NMR (CD_3COCD_3): δ 1.02 (3H, t, $^3J_{H-H} = 6.9$ Hz, Me (NEt)), 1.22 (3H, s, Me (alkenyl)), 1.44 (6H, t, $^3J_{H-H} = 6.9$ Hz, Me (NEt)), 2.82 (3H, s, OMe), 3.32 (3H, s, OMe), 2.4−3.7 (8H, m, CH_2 (NEt) and CH_2-CH_2), 5.26 (5H, s, Cp), 7.48−7.63 (6H, m, *m*- and *p*-Ph), 7.6−7.9 (4H, m, *o*-Ph). $^{31}P\{^1H\}$ NMR (CD_3COCD_3): δ 44.9 (s, $^1J_{Pt-P} = 4010$ Hz). IR (KBr, cm^{-1}): 1664 (s), 1685 (s), 1739 (s), 1917 (s).

($Ph_2PC_2H_4NEt_2$-κ^1*P*)(CO){μ-MeO_2C(Me)C=CCO_2Me}Pt−MoCp(μ-CO)(CO) (9). Complex **8** (12.7 mg, 0.0221 mmol) was placed in an NMR tube, and CD_3COCD_3 (0.6 mL) was added by vacuum distillation. Then CO (1 atm) was introduced into the NMR tube. Complex **9** was characterized spectroscopically. Yield: 50%. ^1H NMR (CD_3COCD_3): δ 0.90 (6H, t, $^3J_{H-H} = 6.9$ Hz, Me (NEt)), 1.67 (3H, s, Me (alkenyl)), 2.50 (4H, q, $^3J_{H-H} = 6.9$ Hz, CH_2 (NEt)), 2.5−3.0 (4H, m, CH_2CH_2), 3.19 (3H, s, OMe), 3.43 (3H, s, OMe), 5.37 (5H, s, Cp), 7.5−7.7 (10H, m, Ph). $^{31}P\{^1H\}$ NMR (CD_3COCD_3): δ 15.4 (s, $^1J_{Pt-P} = 3136$ Hz).

($Ph_2PC_2H_4NEt_2$-κ^1*P*)(^{t}BuNC)MePt{μ-η^2,η^2-C(O)C_2(CO_2Me)$_2$}MoCp(μ-CO)(CO) (10). To a solution of **5** (55.5 mg, 0.0629 mmol) in acetone was added ^{t}BuNC (10 μL, 0.088 mmol) at −30 °C, and the solution was stirred for a few hours. The solution was evaporated under reduced pressure and recrystallized from acetone/hexane in the presence of an excess amount of ^{t}BuNC to give yellow crystals. Yield: 35% (21.0 mg, 0.0220 mmol). Anal. Calcd for $C_{38}H_{47}MoN_2O_7PPt$: C, 47.26; H, 4.91; N, 2.90. Found: C, 47.17; H, 4.87; N, 3.08. Molar electrical conductivity Λ (THF, 24 °C): 0.050 S $cm^2\ mol^{-1}$. ^1H NMR (CD_3COCD_3): δ 0.81 (6H, t, $^3J_{H-H} = 6.9$ Hz, Me (N−Et)), 0.83 (3H, d, $^3J_{P-H} = 6.3$ Hz, Pt−Me), 1.25 (9H, s, Me (^{t}Bu)), 2.37 (4H, q, $^3J_{H-H} = 6.9$ Hz CH_2 (N−Et)), 2.1−2.9 (4H, m, CH_2CH_2), 3.52 (3H, s, OMe), 3.72 (3H, s, OMe), 5.36 (5H, s, Cp), 7.44−7.72 (10H, m, Ph). $^{31}P\{^1H\}$ NMR (CD_3COCD_3): δ −12.1 (s, $^1J_{Pt-P} = 2348$ Hz). IR (KBr, cm^{-1}): 1682 (s), 1700 (s), 1783 (s), 1959 (s), 2200 (s).

($Ph_2PC_2H_4NEt_2$-κ^1*P*)(PMe_3)MePt{μ-η^2:η^2-C(O)C_2(CO_2Me)$_2$}MoCp(μ-CO)(CO) (11). To a solution of **5** (107.9 mg, 0.1222 mmol) in toluene was added PMe_3 (15 μL, 0.14 mmol) at −30 °C, and the solution was stirred for 5 h at −30 °C. Then, the solution was concentrated under reduced pressure at −30 °C, and excess hexane was added to give a yellow powder. Yield: 67% (78.7 mg, 0.0821 mmol). ^1H NMR (CD_3COCD_3): δ 0.70 (3H, d, $^3J_{P-H} = 6.0$, 9.3 Hz, Pt−Me), 0.80 (6H, t, $^3J_{H-H} = 6.9$ Hz, Me (N−Et)), 0.92 (9H, d, $^2J_{P-H} = 5.1$ Hz, Me (PMe_3)), 2.2−3.1 (4H, m, CH_2CH_2), 2.35 (4H, q, $^3J_{H-H} = 6.9$ Hz CH_2 (N−Et)), 3.46 (3H, s, OMe), 3.67 (3H, s, OMe), 5.45 (5H, s, Cp), 7.4−7.7 (10H, m, Ph). $^{31}P\{^1H\}$ NMR (CD_3COCD_3): δ −52.6 (d, $^2J_{P-P} = 13$ Hz, $^1J_{Pt-P} = 1156$ Hz), −16.9 (d, $^2J_{P-P} = 13$ Hz, $^1J_{Pt-P} = 2310$ Hz). IR (KBr, cm^{-1}): 1695 (s), 1776 (vs), 1952 (vs).

($Ph_2PC_2H_4NEt_2$-κ^2*N,P*){μ-MeO_2C($BuHNCO$)C=CCO_2Me}-Pt−MoCp(μ-CO)(CO) (12). Complex **5** (12.6 mg, 0.0142 mmol) was placed in an NMR tube into which C_6D_6 was added by vacuum distillation. The NMR tube was capped with a rubber septum under a nitrogen atmosphere, and then NH_2-Bu (1.4 μL, 0.014 mmol) was injected into the NMR tube by use of a hypodermic syringe. Complex **12** was characterized spectroscopically. Yield: 90%. ^1H NMR (C_6D_6): δ 0.71 (3H, t, $^3J_{H-H} = 6.9$ Hz, Me (NEt)), 0.80 (3H, t, $^3J_{H-H} = 7.4$ Hz, Me (Bu)), 1.06 (3H, t, $^3J_{H-H} = 6.8$ Hz, Me (NEt)), 1.30 (2H, m, CH_2 (Bu)), 1.45 (2H, q, $^3J_{H-H} = 6.9$ Hz, CH_2 (Bu)), 1.7−2.2 (4H, m, CH_2CH_2), 2.33 (1H, m, CH_2 (NEt)), 2.80 (3H, s, OMe), 3.17 (3H, s, OMe), 3.29 (4H, m, CH_2 (NEt) and CH_2 (Bu)), 3.57 (1H, m, CH_2 (NEt)), 5.28 (5H, s, Cp), 7.20 (6H, m, *m*- and *p*-Ph), 7.85 (4H, m, *o*-Ph). $^{31}P\{^1H\}$ NMR (C_6D_6): δ 40.3 (s, $^1J_{Pt-P} = 4497$ Hz).

($Ph_2PC_2H_4NEt_2$-κ^2*N,P*){μ-MeO_2C(Et_2NCO)C=CCO_2Me}-Pt−MoCp(μ-CO)(CO) (13). To a solution of **5** (113 mg, 0.129 mmol) in THF was added $NHEt_2$ (20 μL, 0.19 mmol) and the mixture was stirred for 5 h at ambient temperature. All the volatile matters were removed by evaporation and the resulting solid was extracted with hexane. The hexane solution was evaporated to dryness and the resulting yellow solid of **13** was dried under vacuum. Yield 31% (383 mg, 0.0408 mmol). Anal. Calcd for $C_{36}H_{45}MoN_2O_7PPt$: C, 46.01; H, 4.83; N, 2.98. Found: C, 45.96; H, 4.96; N, 3.0. ^1H NMR (C_6D_6): δ 0.84 (3H, t, $^3J_{H-H} = 7.2$ Hz, Me (NEt)), 0.93 (3H, t, $^3J_{H-H} = 7.2$ Hz, Me (NEt)), 1.06 (3H, br, Me (CONEt)), 1.13 (3H, br, Me (CONEt)), 1.7−2.4 (4H, m, CH_2−CH_2), 2.60 (1H, dq, $^3J_{H-H} = 7.2$ Hz, $^2J_{H-H} = 13.2$ Hz, CH_2 (NEt)), 2.78 (1H, dq, $^3J_{H-H} = 7.2$ Hz, $^2J_{H-H} = 13.2$ Hz, CH_2 (NEt)), 2.91 (3H, s, OMe), 3.35 (2H, m, CH_2 (NEt)), 3.3−3.6 (3H, br, CH_2 (CONEt)), 3.52 (3H, s, OMe), 3.95 (1H, br, CH_2 (CONEt)), 5.35 (5H, s, Cp), 7.0−7.9 (10H, m, Ph). $^{31}P\{^1H\}$ NMR (C_6D_6): δ 39.6 (s, $^1J_{Pt-P} = 4298$ Hz). IR (KBr, cm^{-1}): 1618 (s), 1670, (s) 1687 (s), 1715 (s), 1958 (s).

($Ph_2PC_2H_4NEt_2$-κ^2*N,P*){μ-MeO_2C(C_4H_8NCO)C=CCO_2Me}-Pt−MoCp(μ-CO)(CO) (14). Complex **5** (18.3 mg, 0.0207 mmol) was placed in an NMR tube into which C_6D_6 was added by vacuum distillation. The NMR tube was capped with a rubber septum under a nitrogen atmosphere, and then pyrrolidine (1.8 μL, 0.022 mmol) was injected into the NMR tube by use of a hypodermic syringe. Complex **14** was characterized spectroscopically. Yield: 96%. ^1H NMR (C_6D_6): δ 0.86 (3H, t, $^3J_{H-H} = 6.8$ Hz, Me (NEt)), 0.95 (3H, t, $^3J_{H-H} = 7.0$ Hz, Me

(NEt)), 1.2−1.6 (4H, m, CH_2CH_2 (NC_4H_8)), 1.7−2.4 (4H, m, CH_2CH_2), 2.6−2.9 (2H, m, CH_2 (NEt)), 2.89 (3H, s, OMe), 3.1−3.6 (5H, m, CH_2 (NEt) and CH_2 (NC_4H_8)), 3.53 (3H, s, OMe), 3.95 (1H, m, CH_2 (NC_4H_8)), 5.34 (5H, s, Cp), 7.0−7.4 (6H, m, *m*- and *p*-Ph), 7.8−8.0 (4H, m, *o*-Ph). $^{31}P\{^1H\}$ NMR (C_6D_6): δ 38.6 (s, $^1J_{Pt-P}$ = 4365 Hz).

Hydrogenolysis of 13 and 14. Treatment of **13** (5.4 mg, 0.0057 mmol) with hydrogen gas (1 atm) at ambient temperature for 2 days in C_6D_6 gave $MeO_2CCH_2CH(CONEt_2)CO_2Me$ (86%), which was confirmed by direct comparison with an authentic sample prepared independently from $MeO_2CCH_2CONEt_2$ (1.0971 g, 6.3339 mmol), potassium carbonate (842.8 mg, 6.098 mmol), tetra-*n*-butylammonium bromide (38.4 mg, 0.119 mmol), and methyl bromoacetate (520 μL, 5.49 mmol) in benzene (12%). MS: *m*/*z* 245 (M^+), 214 (M^+ − OMe), 186 (M^+ − CO_2Me), 145 (M^+ − $CONEt_2$). ^1H NMR (C_6D_6): δ 0.92 (3H, t, $^3J_{H-H}$ = 6.6 Hz, CH_3), 0.94 (3H, t, $^3J_{H-H}$ = 6.9 Hz, CH_3), 2.9−3.2 (6H, CH_2), 4.01 (1H, t, $^3J_{H-H}$ = 6.9 Hz, C*H*).

Treatment of **14**, prepared in situ from **5** and pyrrolidine, with hydrogen gas (1 atm) at ambient temperature in C_6D_6 gave $MeO_2CCH_2CH(CONC_4H_8)CO_2Me$, which was characterized by GC-MS: *m*/*z* 243 (M^+), 212 (M^+ − OMe), 184 (M^+ − CO_2Me), 145 (M^+ − $CONC_4H_8$).

K^+[($Ph_2PC_2H_4NEt_2$-κ^1*P*)Me{μ-$MeO_2C(PhO_2C)C{=}CCO_2Me$}Pt−MoCp($\mu$-CO)(CO)]$^-$ (15). A solution of KOPh (222 mg, 0.167 mmol) in THF was added dropwise to a THF solution of **6** (51.3 mg, 0.0581 mmol) at −30 °C, and the resulting mixture was stirred for 3 h at −30 °C. The mixture was further stirred for 30 min at ambient temperature; the reaction mixture was then evaporated to dryness, and the resulting solid was extracted with benzene. After concentration of the extract, a small amount of hexane was added and the mixture was cooled to −30 °C to give complex **15** as dark red crystals. Yield: 89% (52.6 mg, 0.0518 mmol). Anal. Calcd for $C_{39}H_{43}KMoNO_8PPt$: C, 46.16; H, 4.27; N, 1.38. Found: C, 46.29; H, 4.12; N, 1.35. Molar electrical conductivity Λ (THF, 20 °C): 0.77 S cm^2 mol^{-1}. ^1H NMR (CD_3COCD_3): δ 0.25 (3H, d, $^3J_{P-H}$ = 8.2 Hz, $^2J_{Pt-H}$ = 78.7 Hz, Pt−Me), 0.86 (6H, t, $^3J_{H-H}$ = 7.2 Hz, Me (NEt)), 2.41 (4H, q, $^3J_{H-H}$ = 7.2 Hz, CH_2 (NEt)), 2.4−2.8 (4H, m, CH_2CH_2), 3.45 (3H, s, OMe), 3.55 (3H, s, OMe), 4.93 (5H, s, Cp), 7.0−7.7 (15H, m, Ph). $^{31}P\{^1H\}$ NMR (CD_3COCD_3): δ 19.9 (s, $^1J_{Pt-P}$ = 3038 Hz). IR (KBr, cm^{-1}): 1592 (s), 1661 (s), 1677 (s), 1710 (s), 1919 (s).

Reaction of 15 with MeI. Complex **15** (8.2 mg, 0.0081 mmol) was placed in an NMR tube into which CD_3COCD_3 was added by vacuum distillation. The NMR tube was capped with a rubber septum under a nitrogen atmosphere, and then MeI (1.0 μL, 0.016 mmol) was injected into the NMR tube by use of a hypodermic syringe. ($Ph_2PC_2H_4NEt_2$-κ^2*N*,*P*)Me_2{μ-$MeO_2C(PhO_2C)C{=}CCO_2Me$}Pt−MoCp($\mu$-CO)(CO) (**16**) was characterized spectroscopically. Yield: 95%. ^1H NMR (CD_3COCD_3): δ 0.33 (3H, d, $^3J_{P-H}$ = 7.5 Hz, $^2J_{Pt-H}$ = 75.1 Hz, Pt−Me), 0.79 (3H, t, $^3J_{H-H}$ = 7.5 Hz, Me (NEt)), 0.87 (3H, t, $^3J_{H-H}$ = 7.1 Hz, Me (NEt)), 0.99 (3H, d, $^3J_{P-H}$ = 6.9 Hz, $^2J_{Pt-H}$ = 67.9 Hz, Pt−Me), 2.4−2.7 (2H, m, CH_2CH_2), 3.0−3.3 (6H, m, CH_2 (NEt) and CH_2CH_2), 3.64 (3H, s, OMe), 3.77 (3H, s, OMe), 5.37 (5H, s, Cp), 7.2−7.8 (15H, m, Ph). $^{31}P\{^1H\}$ NMR (CD_3COCD_3): δ −2.4 (s, $^1J_{Pt-P}$ = 2105 Hz). IR (KBr, cm^{-1}): 1543 (s), 1703 (s), 1744 (s), 1925 (vs).

Protonolysis of 15. Complex **15** (4.2 mg, 0.0042 mmol) was placed in an NMR tube into which CD_3COCD_3 was added by vacuum distillation. The NMR tube was capped with a rubber septum under a nitrogen atmosphere, and then 1.7 M of HCl/CH_3COCH_3 (2.6 μL, 0.0044 mmol) was injected into the NMR tube by use of a hypodermic syringe. Methane was detected in 106% yield. ($Ph_2PC_2H_4NEt_2$-κ^2*N*,*P*){μ-$MeO_2C(PhO_2C)C{=}C$-CO_2Me}Pt−MoCp(μ-CO)(CO) (**17**) was characterized spectroscopically. Yield: 98%. ^1H NMR (CD_3COCD_3): δ 0.88 (3H, t, $^3J_{H-H}$ = 7.2 Hz, Me (NEt)), 1.31 (3H, t, $^3J_{H-H}$ = 7.2 Hz, Me (NEt)), 2.4−2.7 (2H, m, CH_2CH_2), 3.0−3.3 (6H, m, CH_2 (NEt) and CH_2CH_2), 3.01 (3H, s, OMe), 3.53 (3H, s, OMe), 5.22 (5H, s, Cp), 6.70 (1H, m, *p*-Ph (CO_2Ph)), 7.0−7.3 (4H, m, *o*- and *m*-Ph (CO_2Ph)), 7.5−7.8 (10H, m, Ph (PPh)). $^{31}P\{^1H\}$ NMR (CD_3COCD_3): δ 43.1 (s, $^1J_{Pt-P}$ = 4139 Hz).

Table 4. Crystallographic Parameters for 5, 8, and 10

	5	**8**	**10**
empirical formula	$C_{33}H_{38}MoNO_7PPt$	$C_{32}H_{38}MoNO_6PPt$	$C_{38}H_{47}MoN_2O_7PPt$
formula wt	882.67	854.66	965.80
cryst syst	monoclinic	orthorhombic	triclinic
space group	$P2_1/n$ (No. 14)	$P2_12_12_1$ (No. 19)	$P\bar{1}$ (No. 2)
a (Å)	12.235(6)	15.239(2)	13.12(2)
b (Å)	20.712(5)	15.717(3)	15.35(1)
c (Å)	14.634(3)	12.894(2)	11.31(1)
α (deg)			93.55(9)
β(deg)	109.53(2)		116.29(10)
γ(deg)			76.2(1)
V (Å^3)	3494(2)	3088.3(8)	1980(4)
Z	4	4	2
D_{calcd} (g/cm^3)	1.677	1.838	1.619
F_{000}	1736.00	1680.00	960.00
μ(Mo Kα) (cm^{-1})	44.31	50.09	39.17
radiation	Mo Kα (λ= 0.710 69 Å), graphite monochromated		
scan type	ω−2θ	ω−2θ	ω−2θ
$2\theta_{max}$ (deg)	54.9	55.0	55.1
no. of rflns measd			
total	8440	3973	9398
unique	7842	3948	9058
structure soln	direct methods (SIR92)		
no. of observns ($I > 3.00\sigma(I)$)	4237	3417	7209
no. of variables	362	379	451
residuals: *R*;[a] R_w[b]	0.064; 0.121	0.027; 0.038	0.060; 0.083
goodness of fit indicator	1.29	1.08	1.08

[a] $R = \sum||F_o| - |F_c||/\sum|F_o|$. [b] $R_w = [\sum w(|F_o| - |F_c|)^2/\sum wF_o^2]^{1/2}$.

X-ray Structure Analysis. A single crystal was selected by using a microscope and sealed in a thin-glass capillary (GLASS, 0.7 mm i.d.) under N_2. Diffraction experiments were performed on a Rigaku RASA-7R diffractometer with graphite-monochromated Mo Kα radiation (λ = 0.710 69 Å) and a rotating anode generator. The intensities of 3 representative reflections were measured after every 150 reflections. No intensity decay was observed for **8**. For complexes **5** and **10**, a small intensity decay was observed, 6.2 and 9.1%, respectively, and decay corrections were applied. These structures were solved by direct methods[16] expanded using Fourier techniques,[17] and refined by full-matrix least squares. For complex **5**, all non-hydrogen atoms were refined with anisotropic displacement parameters except for C19 and C21−C26, and all hydrogen atoms were included in theoretical positions. For **8** and **10**, all non-hydrogen atoms were refined anisotropically, and the hydrogen atoms were included in theoretical positions. For complex **15**, single crystals were obtained from diethyl ether, but the crystals rapidly degradated under vacuum. Therefore, a single crystal was carefully mounted in a glass capillary tube. However, sufficient diffraction data could not be obtained due to extensive signal intensity decay (33.4%, $2\theta_{max}$ = 40.0°), and only a brief structural feature was discussed in the text. Crystal data for **15**·Et_2O: $C_{43}H_{53}KMoNO_9PPt$, FW = 1089.00, triclinic, $P\bar{1}$, *a* = 16.430(6) Å, *b* = 16.882(4) Å, *c* = 10.530(3) Å, α = 101.34(2)°, β = 106.64-(3)°, γ = 71.23(2)°, *V* = 2631(1) Å^3, Z = 2, D_{calcd} = 1.374 g cm^{-3}, μ(Mo Kα) = 30.36 cm^{-1}, $2\theta_{max}$ = 40.0°, 4950 reflections

(16) SIR92: Altomare, A.; Burla, M. C.; Camalli, M.; Cascarano, M.; Giacovazzo, C.; Guagliardi, A.; Polidori, G. *J. Appl. Crystallogr.* **1994**, *27*, 435.

(17) DIRDIF94: Beurskens, P. T.; Admiraal, G.; Beurskens, G.; Bosman, W. P.; de Gelder, R.; Israel, R.; Smits, J. M. M. 1994. The DIRDIF-94 Program System; Technical Report of the Crystallography Laboratory; University of Nijmegen, Nijmegen, The Netherlands.

measured (4718 unique), 3704 observations with $I > 3.00\sigma(I)$, R (R_w) = 0.059 (0.091), GOF = 1.01. Selected bond distances (Å): Pt(1)−Mo(1) = 2.792(2), Pt(1)−P(1) = 2.272(5), Pt(1)−C(1) = 2.10(2), Pt(1)−C(2) = 2.04(1), Pt(1)−C(33) = 2.16(2), Mo(1)−C(2) = 2.14(2), Mo(1)−C(5) = 2.32(2), Mo(1)−C(33) = 1.98(2) Å. Selected bond angles (deg): Mo(1)−Pt(1)−P(1) = 131.8(1), Mo(1)−Pt(1)−C(1) = 141.0(5), Mo(1)−Pt(1)−C(2) = 49.6(4), Mo(1)−Pt(1)−C(33) = 44.9(6), P(1)−Pt(1)−C(1) = 87.1-(5), P(1)−Pt(1)−C(2) = 173.2(4), P(1)−Pt(1)−C(33) = 91.4(6), C(1)−Pt(1)−C(2) = 91.5(7), C(1)−Pt(1)−C(33) = 161.5(7), C(2)−Pt(1)−C(33) = 92.1(7), Pt(1)−C(33)−Mo(1) = 84.6(8), Pt-(1)−C(33)−O(7) = 126(1), Mo(1)−C(33)−O(7) = 148(1).

These data were processed using the *teXsan* crystal solution package[18] operating on a SGI O_2 workstation. The crystallographic data and details associated with data collection for **5**, **8**, and **10** are given in Table 4. Crystallographic thermal parameters and bond distances and angles have been deposited as Supporting Information.

(18) teXsan: Crystal Structure Analysis Package; Molecular Structure Corp., The Woodlands, TX, 1985 and 1999.

Acknowledgment. This work was financially supported by a Grant-in-Aid for Scientific Research from the Ministry of Education, Sports, Culture, Science and Technology of Japan and the 21st Century COE (Center of Excellence) program of "Future Nano-materials" at the Tokyo University of Agriculture and Technology.

Supporting Information Available: Tables of atomic coordinates, anisotropic displacement parameters, and bond distances and angles for **5**, **8**, **10**, and **15**. This material is available free of charge via the Internet at http://pubs.acs.org.

OM034162Q